A Multi-Model Assessment of Regional Climate Disparities Caused by Solar Geoengineering (Supplemental Online Material)

Ben Kravitz*[1], Douglas G. MacMartin[2,3], Alan Robock[4], Philip J. Rasch[1], Katharine L. Ricke[3], Jason N. S. Cole[5], Charles L. Curry[6], Peter J. Irvine[7], Duoying Ji[8], David W. Keith[9], Jón Egill Kristjánsson[10], John C. Moore[8], Helene Muri[10], Balwinder Singh[1], Simone Tilmes[11], Shingo Watanabe[12], Shuting Yang[13], and Jin-Ho Yoon[1]

[1]Atmospheric Sciences and Global Change Division, Pacific Northwest National Laboratory, Richland, WA.

[2]Department of Computing and Mathematical Sciences, California Institute of Technology, Pasadena, CA.

[3]Department of Global Ecology, Carnegie Institution for Science, Stanford, CA.

[4]Department of Environmental Sciences, Rutgers University, New Brunswick, NJ.

[5]Canadian Centre for Climate Modeling and Analysis, Environment Canada, Toronto, Ontario, Canada.

[6]School of Earth and Ocean Sciences, University of Victoria, Victoria, British Columbia, Canada.

[7]IASS Institute for Advanced Sustainability Studies, Potsdam, Germany.

[8]State Key Laboratory of Earth Surface Processes and Resource Ecology, College of Global Change and Earth System Science, Beijing Normal University, Beijing, China.

[9]School of Engineering and Applied Sciences, Harvard University, Cambridge, MA.

[10]Department of Geosciences, University of Oslo, Oslo, Norway.

[11]National Center for Atmospheric Research, Boulder, CO.

[12]Japan Agency for Marine-Earth Science and Technology, Yokohama, Japan.

[13]Danish Meteorological Institute, Copenhagen, Denmark.

*To whom correspondence should be addressed; Ben Kravitz, P. O. Box 999, MSIN K9-24, Richland, WA 99352, USA; E-mail: ben.kravitz@pnnl.gov.

1 Simulation Choice and Linearity

In this paper, we use the abrupt4xCO2 simulation from CMIP5 and the G1 simulation from GeoMIP (Taylor *et al* 2012; Kravitz *et al* 2011), both of which are highly idealized. abrupt4xCO2 involves an instantaneous quadrupling of the CO_2 concentration from preindustrial levels. G1 involves a reduction in solar irradiance to counteract the radiative forcing in abrupt4xCO2. Despite these experiments being idealized, we argue that our analysis provides useful conclusions regarding modeled effects of solar geoengineering and that our choice of simulations strengthens our conclusions.

The continuously varying forcings in the Representative Concentration Pathway (RCP) scenarios can be viewed as the sum of a series of step changes in forcing, similar to the concept of a Riemann integral. As such, abrupt-style simulations have broader applicability to more "realistic" simulations. Good *et al* (2012, 2013) found that by using such an approach, re-scaled abrupt-style simulations can capture the patterns of change of global mean temperature, precipitation, and ocean heat uptake. The radiative forcing and climate response of abrupt increases in CO_2 are known to be nonlinear with the magnitude of the forcing, so scaling the modeled effects in an abrupt-style simulation to the levels of forcing in an RCP simulation is not entirely accurate. However, these nonlinearities are secondary as compared to inter-model spread in determining radiative forcing and climate response in these simulations (Andrews *et al* 2012). These assertions may not be true for significantly larger abrupt CO_2 forcings, but they hold within the range of forcings considered in our study.

In G1, feedbacks related to global-mean temperature changes are suppressed (Kravitz *et al* 2013), meaning nonlinearities in climatic response in G1 are quite small. Furthermore, abrupt4xCO2 and G1 have high local signal-to-noise ratios, making these simulations ideal for determining modeled climate response to solar geoengineering (Kravitz *et al* 2013). This approach may not hold for variables other than temperature and precipitation due to potentially nonlinear behavior, including tipping point thresholds that may not be well represented by climate models (Lenton *et al* 2008).

The simulated method of solar geoengineering, i.e., reducing solar irradiance, is not a realistic representation of all possible uniform solar geoengineering methods. However, this representation has been shown to capture the broad features of modeled temperature and precipitation responses to those of a layer of stratospheric sulfate aerosols (Ammann *et al* 2010; Niemeier *et al* 2013). As such, we are confident that the results of our study are indicative of the response to other methods of uniform solar geoengineering. Notable differences include effects on the biosphere due to changes in the direct-diffuse light balance (Kravitz *et al* 2012) or differences in the exact value of precipitation response (Niemeier *et al* 2013), but these are unlikely to change the sign of the response to the dominant radiative effects.

In Section 2, we described that g ranges between 0 and 2. The choice of 2 as the upper limit for g was arbitrarily chosen as sufficiently large to capture the relevant calculations of the maximum amount of g as determined by the Pareto criterion (Equation 7). Figure 1 shows that for nearly all regions, $g = 2$ is sufficient for this purpose.

In all calculations, we excluded changes which were not statistically significant, i.e., if we did not have confidence in our ability to discern the sign of the change due to either CO_2 increases or solar reductions. For the abrupt4xCO2 simulation, if

$$|D_i(w;0)| < \frac{1.96}{\sqrt{39}}$$

for a region i in a particular model, then we conclude that the climate change due to an abrupt increase in CO_2 is indistinguishable from natural variability, so D in Equations 3-6 are set to 0 for that region. For $g = 1$, if

$$|D_i(w;0) - D_i(w;1)| < \frac{1.96}{\sqrt{39}}$$

for a region i in a particular model, then we conclude that the change due to solar reduction imposed upon an abrupt CO_2 increase is indistinguishable from the change solely due to the CO_2 increase, so $D_i(w;1)$ is set to the same value as $D_i(w;0)$ for that region. The factor of 1.96 indicates a 95% confidence interval based on a normal distribution, and the factor of 39 indicates the number of independent degrees of freedom when using averages over years 11-50 of the simulations.

There may be serial autocorrelation at the interannual time scale for temperature and precipitation, meaning there may be fewer than 39 independent degrees of freedom in our calculations. Tests (not pictured) using 19 degrees of freedom (a decrease in the signal-to-noise ratio by approximately a factor of $\sqrt{2}$) and 9 degrees of freedom (a decrease in the signal-to-noise ratio by approximately a factor of 2) yielded no changes in the main conclusions of the paper. Use of 19 degrees of freedom resulted in fewer regions showing statistically significant changes due to abrupt4xCO2 or solar geoengineering, and 8 of the 22 regions showed more precipitation changes for more solar reduction. Use of 9 degrees of freedom showed similar results to using 19 degrees of freedom, with 5 of the 22 regions showing larger precipitation changes for more solar reduction.

Some modeling groups performed multiple ensemble members of these simulations. In such cases, we performed all calculations for that model on the ensemble mean.

2 Choice of Regions and Time Averaging

The regions defined by Giorgi and Francisco (Giorgi and Francisco 2000), shown in Supplemental Figure 1, are often termed *Giorgi regions*. These geographically defined regions have been used in recent assessments of regional climate change by the IPCC (e.g., Bindoff *et al* 2013; Hartmann *et al* 2013), as well as several past studies of the climate impacts of solar geoengineering (MacMartin *et al* 2013; Moreno-Cruz *et al* 2012; Ricke *et al* 2013). Other choices of regions could include division by climate type, population density, or economic power, for example. However, as long as the regions considered here undergo differential effects due to CO_2 increases and solar geoengineering, the conclusions of our study do not depend on the choice of regions. A similar argument could be made to justify our use of 40-year averages of monthly averaged model output instead of daily output, or for different methods of geoengineering (e.g., marine cloud brightening). For example, although monthly output is less adept at capturing changes in extreme events than daily output, as long as the effects are experienced differentially across regions, our basic conclusions still hold. We primarily chose to use Giorgi regions in this study because their use in geoengineering studies has precedent and has been shown to be useful in revealing important findings regarding the climatic effects of geoengineering (MacMartin *et al* 2013; Moreno-Cruz *et al* 2012; Ricke *et al* 2013).

In Section 2, we claimed that the period of averaging the abrupt4xCO2 temperature and precipitation values would not change the conclusions of our paper. In most of this paper, the temperature and precipitation values were averaged over years 11-50 of the abrupt4xCO2, which is during a period of rapid climate transition. For comparison, we performed calculations in 8 of the 12 models using averages over years 101-140, which is a period of much less rapid climate transition. These results are shown in Supplemental Figure 16. The quantitative values expectedly differ from the values shown in Figure 3 and Supplemental Figure 10, but the conclusions of the paper are unchanged by shifting the averaging period.

We also claim in the text that changing analysis to a seasonal scale would not change the conclusions of our paper. In many of the supplemental figures that follow (specifically, Supplemental Figures 3-6, 8-9, 11-12, and 14-15), we repeat our analyses but for June-July-August and December-January-February averages. Although the individual values of the different quantities do change when using seasonal averages instead of annual averages, the conclusions do not. When considering only temperature, all models in all regions show reduced values of D for a moderate amount of geoengineering. When considering only precipitation, several models show the maximum amount of geoengineering as determined by the Pareto criterion to be $g = 0$, indicating D will increase for any amount of geoengineering.

References

1. Ammann C M, Washington W M, Meehl G A, Buja L, Teng H 2010 Climate engineering through artificial enhancement of natural forcings: Magnitudes and implied consequences *J. Geophys. Res.* **115** D22109 doi:10.1029/2009JD012878

2. Andrews T, Gregory J M, Webb M J, Taylor K E 2012 Forcing, feedbacks and climate sensitivity in CMIP5 coupled atmosphere-ocean climate models *Geophys. Res. Lett.* **39** L09712 doi:10.10292012GL051607

3. Bindoff N L *et al* 2013 Detection and Attribution of Climate Change: from Global to Regional. In *Climate Change 2013: The Physical Science Basis. Contribution of Working Group I to the Fifth Assessment Report of the Intergovernmental Panel on Climate Change* [Stocker T F, Qin D, Plattner G-K, Tignor M, Allen S K, Boschung J, Nauels A, Xia Y, Bex V, Midgley P M (eds.)]. Cambridge University Press, Cambridge, United Kingdom and New York, NY, USA.

4. Giorgi F, Francisco R 2000 Evaluating uncertainties in the prediction of regional climate change *Geophys. Res. Lett.* **27** 1295-1298

5. Good P, *et al* 2012 A step-response approach for predicting and understanding non-linear precipitation changes *Clim. Dynam.* **39** 2789-2803 doi:10.1007/s00382-012-1571-1

6. Good P, Gregory J M, Lowe J A, Andrews T 2013 Abrupt CO_2 experiments as tools for predicting and understanding CMIP5 representative concentration pathway projections *Clim. Dynam.* **40** 1041-1053 doi:10.1007/s00382-012-1410-4

7. Hartmann D L *et al* 2013 Observations: Atmosphere and Surface. In *Climate Change 2013: The Physical Science Basis. Contribution of Working Group I to the Fifth Assessment Report of the Intergovernmental Panel on Climate Change* [Stocker T F, Qin D, Plattner G-K, Tignor M, Allen S K, Boschung J, Nauels A, Xia Y, Bex V, Midgley P M (eds.)]. Cambridge University Press, Cambridge, United Kingdom and New York, NY, USA.

8. Kravitz B *et al* 2011 The Geoengineering Model Intercomparison Project (GeoMIP) *Atmos. Sci. Lett.* **12** 162-167 doi:10.1002/asl.316

9. Kravitz B, MacMartin D G, Caldeira K 2012 Geoengineering: Whiter skies? *Geophys. Res. Lett.* **39** L11801 doi:10.1029/2012GL051652

10. Kravitz B *et al* 2013 Climate model response from the Geoengineering Model Intercomparison Project (GeoMIP) *J. Geophys. Res.* **118** 8302-8332 doi:10.1002/jgrd.50646

11. Lenton T M *et al* 2008 Tipping elements in the Earth's climate system *Proc. Nat. Acad. Sci.* **105** 1786-1793

12. MacMartin D G, Keith D W, Kravitz B, Caldeira K 2013 Managing trade-offs in geoengineering through optimal choice of non-uniform radiative forcing *Nature Climate Change* **3** 365-368 doi:10.1038/nclimate1722

13. Moreno-Cruz J B, Ricke K L, Keith D W 2012 A simple model to account for regional inequalities in the effectiveness of solar radiation management *Climatic Change* **110** 649-668 doi:10.1007/s10584-011-0103-z

14. Niemeier U, Schmidt H, Alterskjær K, Kristjànsson J E 2013 Solar irradiance reduction via climate engineering–Climatic impact of different techniques *J. Geophys. Res.* **118**

11905-11917 doi:10.1002/2013JD020445

15. Ricke K L, Moreno-Cruz J B, Caldeira K 2013 Strategic incentives for climate geoengineering coalitions to exclude broad participation *Environ. Res. Lett.* **8** 014021

16. Taylor K E, Stouffer R J, Meehl G A 2012 An overview of CMIP5 and the experiment design *Bull. Amer. Meteor. Soc.* **93** 485-498 doi:10.1175/BAMS-D-11-00094.1

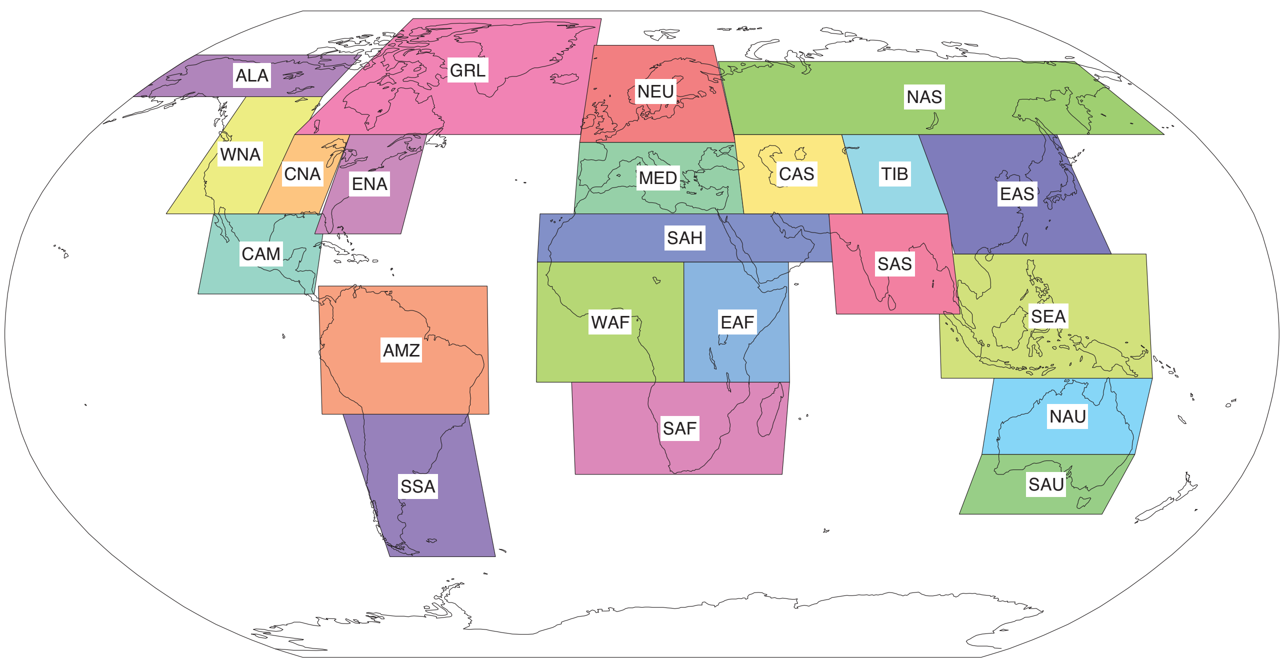

Figure 1: The 22 Giorgi regions considered in this study (Giorgi and Francisco 2000).

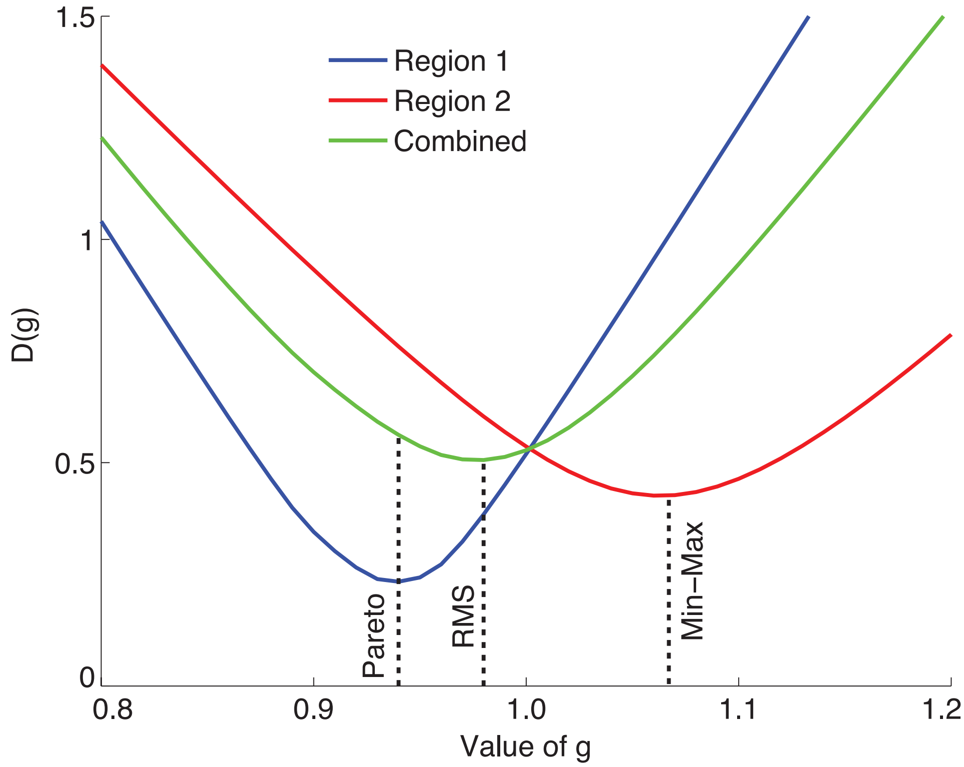

Figure 2: Diagram illustrating three different methods (RMS, Min-Max, Pareto Criterion) of aggregating climate change over regions. Blue and red lines show example values of $D_i(w; g)$ (Equation 3, for any value of w). The value of g that minimizes D for the three methods is shown by dashed lines. The RMS value is given by $\min_{g\geq 0} \sqrt{\frac{1}{22}\sum_{i=1}^{22}\left[D_i(w;g)\right]^2}$. The Min-Max value (improving the worst case) is given by $\min_{g\geq 0}\left[\max_i D_i(w;g)\right]$. The value ascribed to the Pareto criterion described in Equation 7.

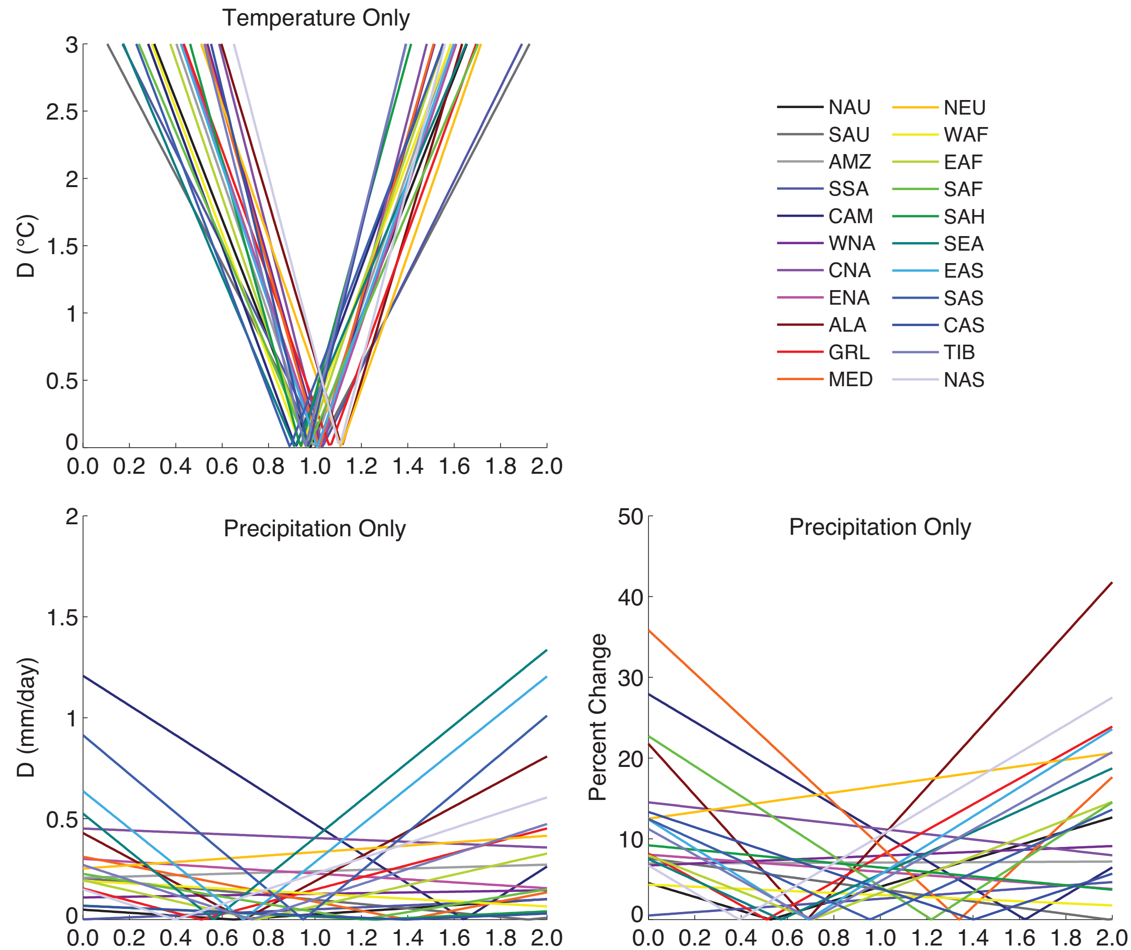

Figure 3: Same as Figure 1 in the main text, but for June-July-August averages.

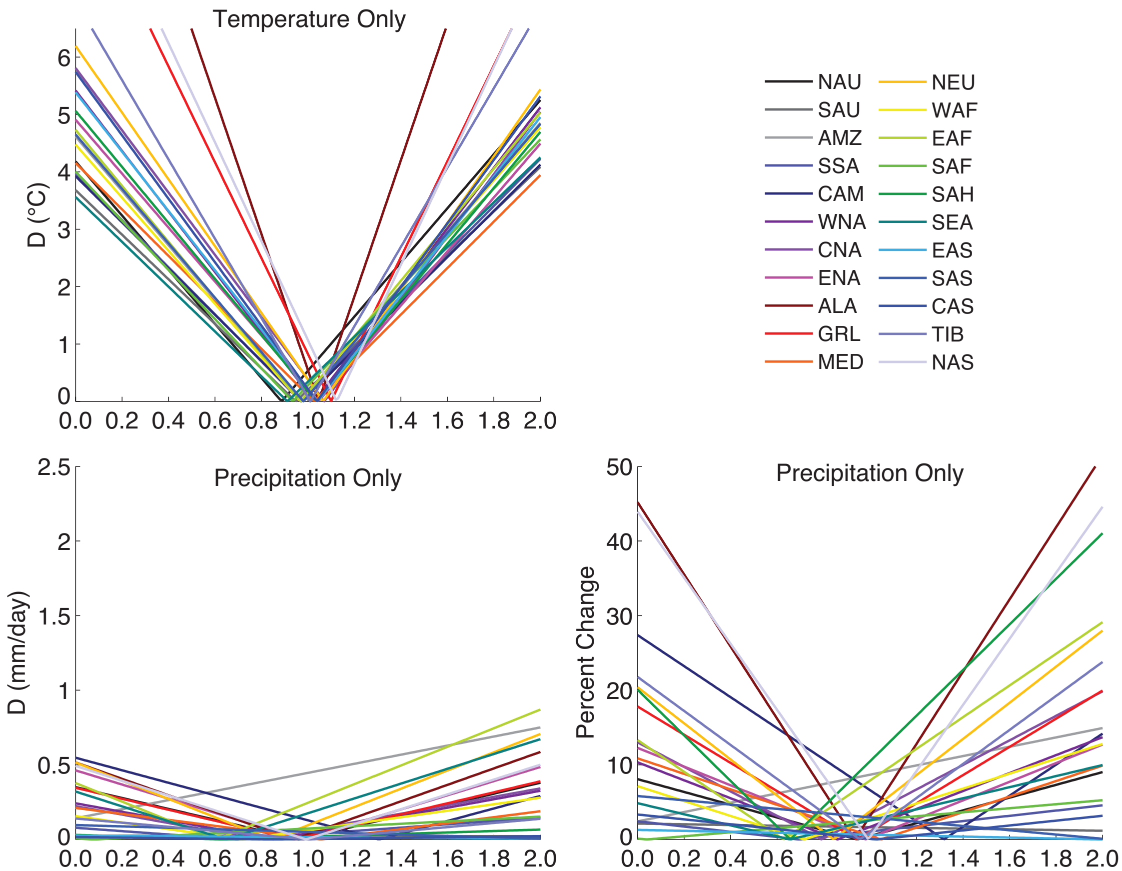

Figure 4: Same as Figure 1 in the main text, but for December-January-February averages.

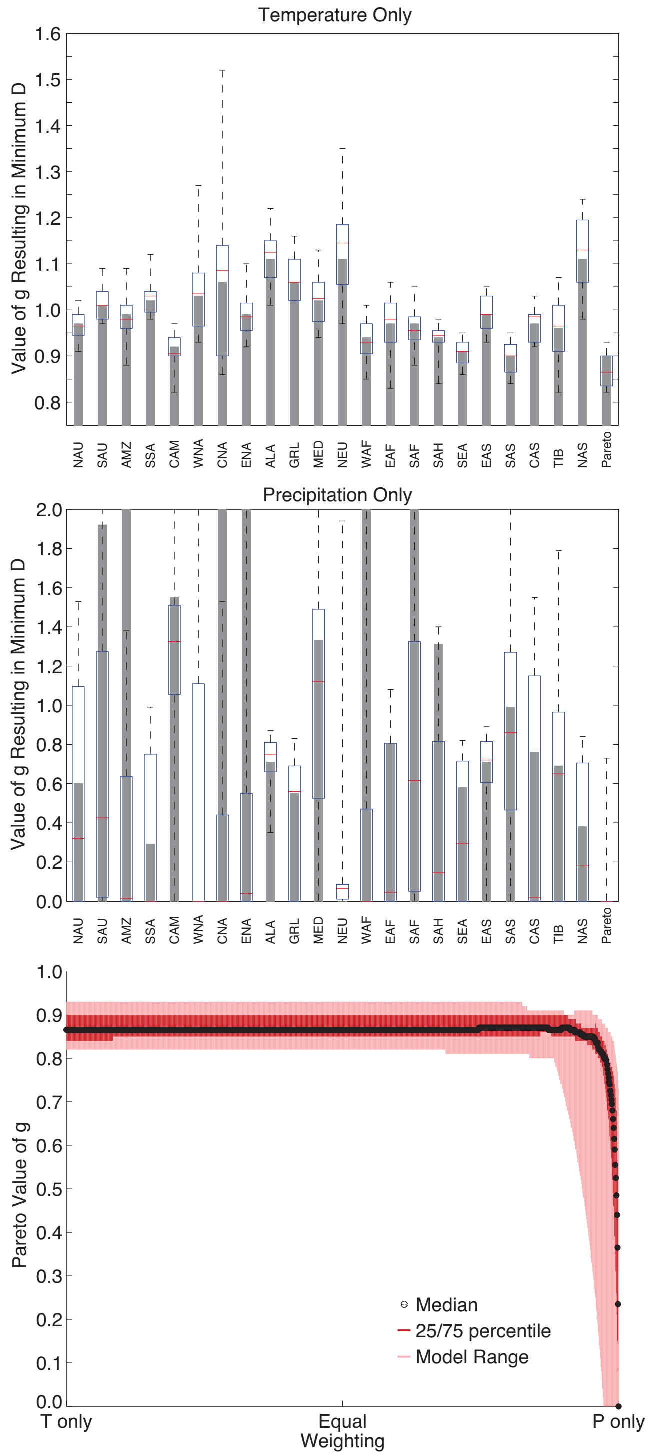

Figure 5: Same as Figures 2 and 3 in the main text, but for June-July-August (JJA) averages. The value of g as determined by the Pareto criterion is slightly lower for all weights than the results for annual averages, but the annual and JJA results are qualitatively similar.

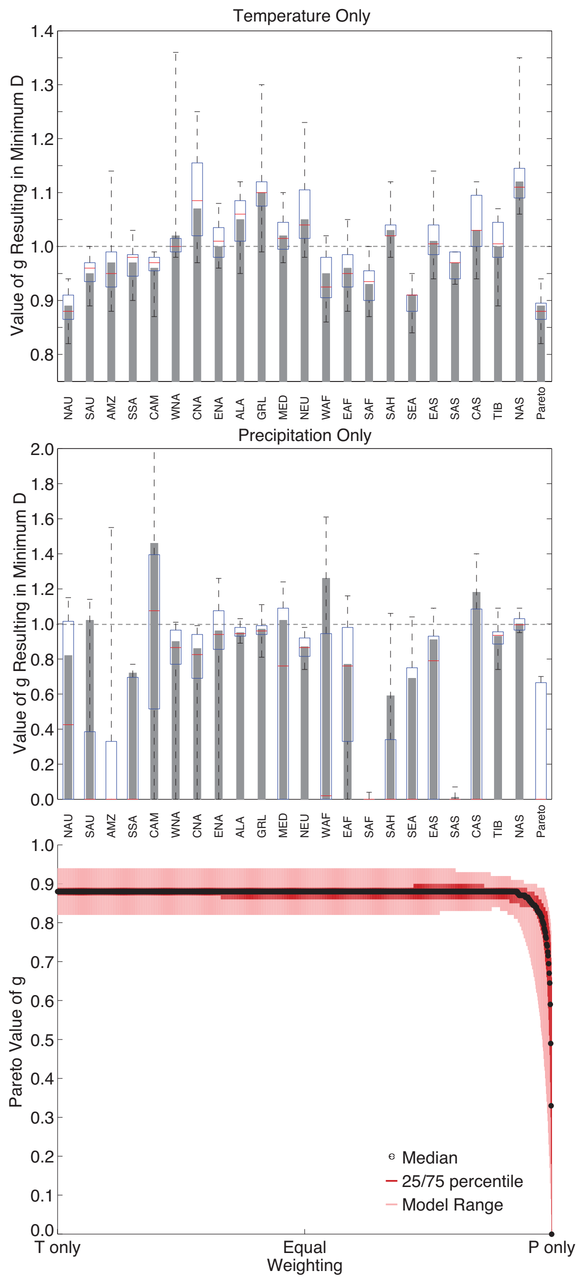

Figure 6: Same as Figures 2 and 3 in the main text, but for December-January-February (DJF) averages. The value of g as determined by the Pareto criterion is slightly lower for all weights than the results for annual averages, but the annual and DJF results are qualitatively similar.

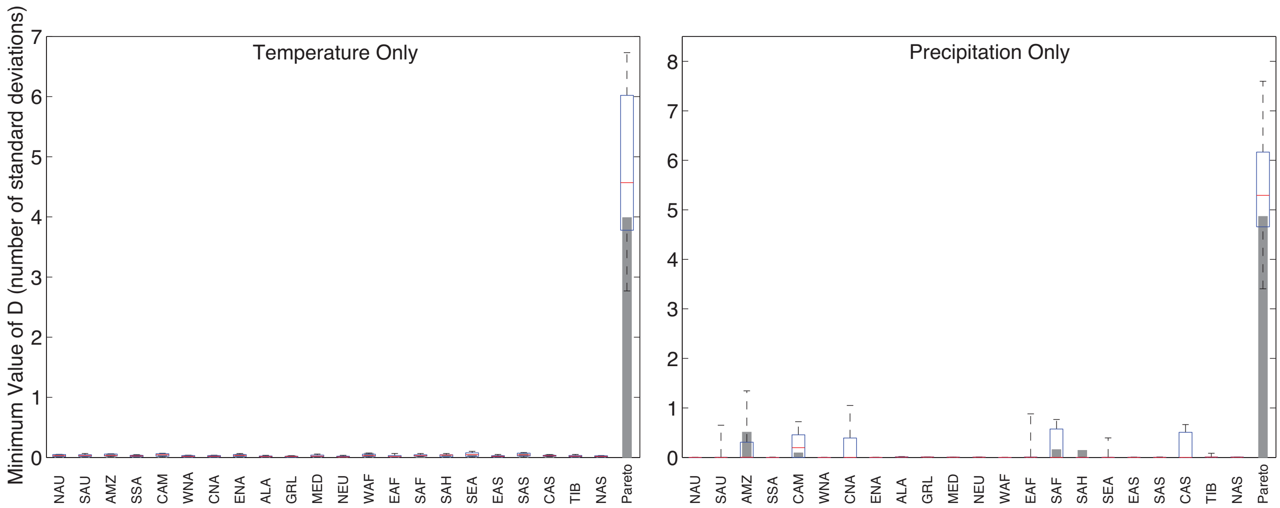

Figure 7: The actual values of D (Equation 3) associated with Figure 2 in the main text. For each individual region, small values of D are achievable if only considering temperature. The same is true for precipitation in most, but not all, regions.

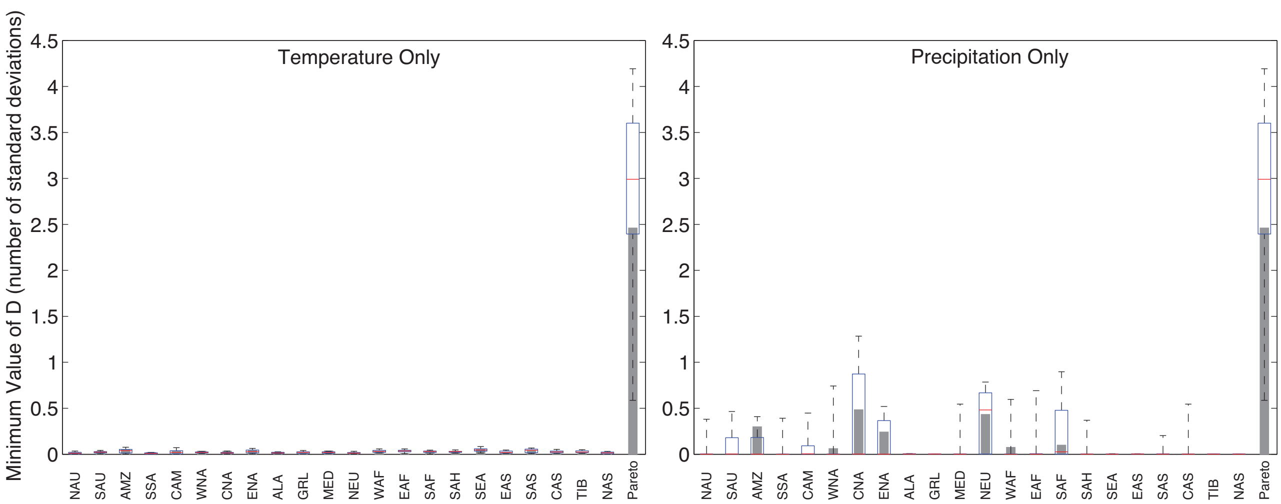

Figure 8: The actual values of D (Equation 3) associated with the top and middle panels of Supplemental Figure 5. For each individual region, small values of D are achievable if only considering temperature. The same is true for precipitation in most, but not all, regions.

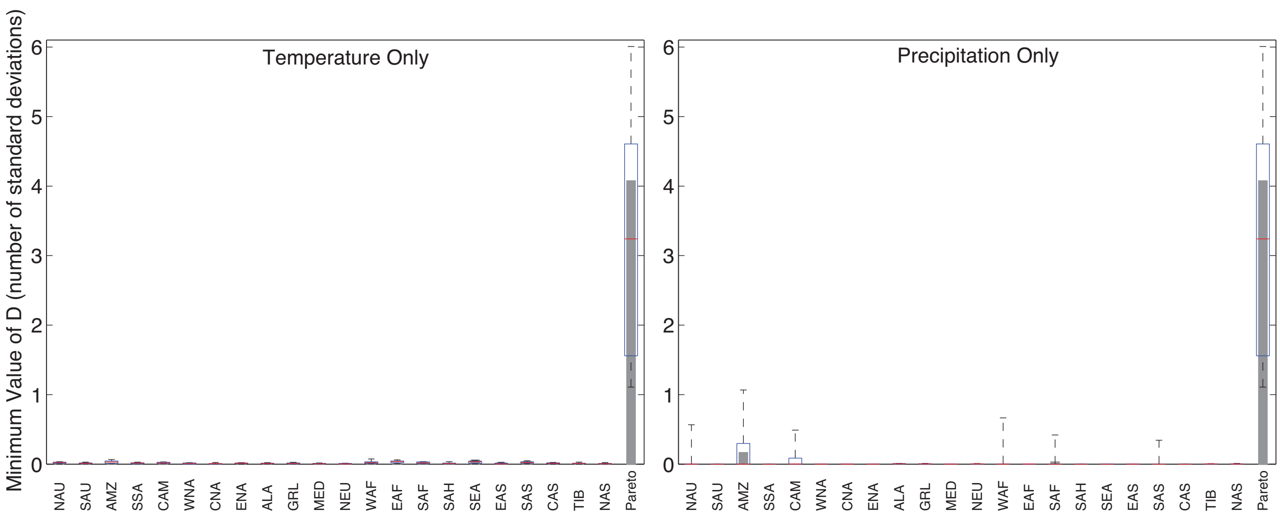

Figure 9: The actual values of D (Equation 3) associated with the top and middle panels of Supplemental Figure 6. For each individual region, small values of D are achievable if only considering temperature. The same is true for precipitation in most, but not all, regions.

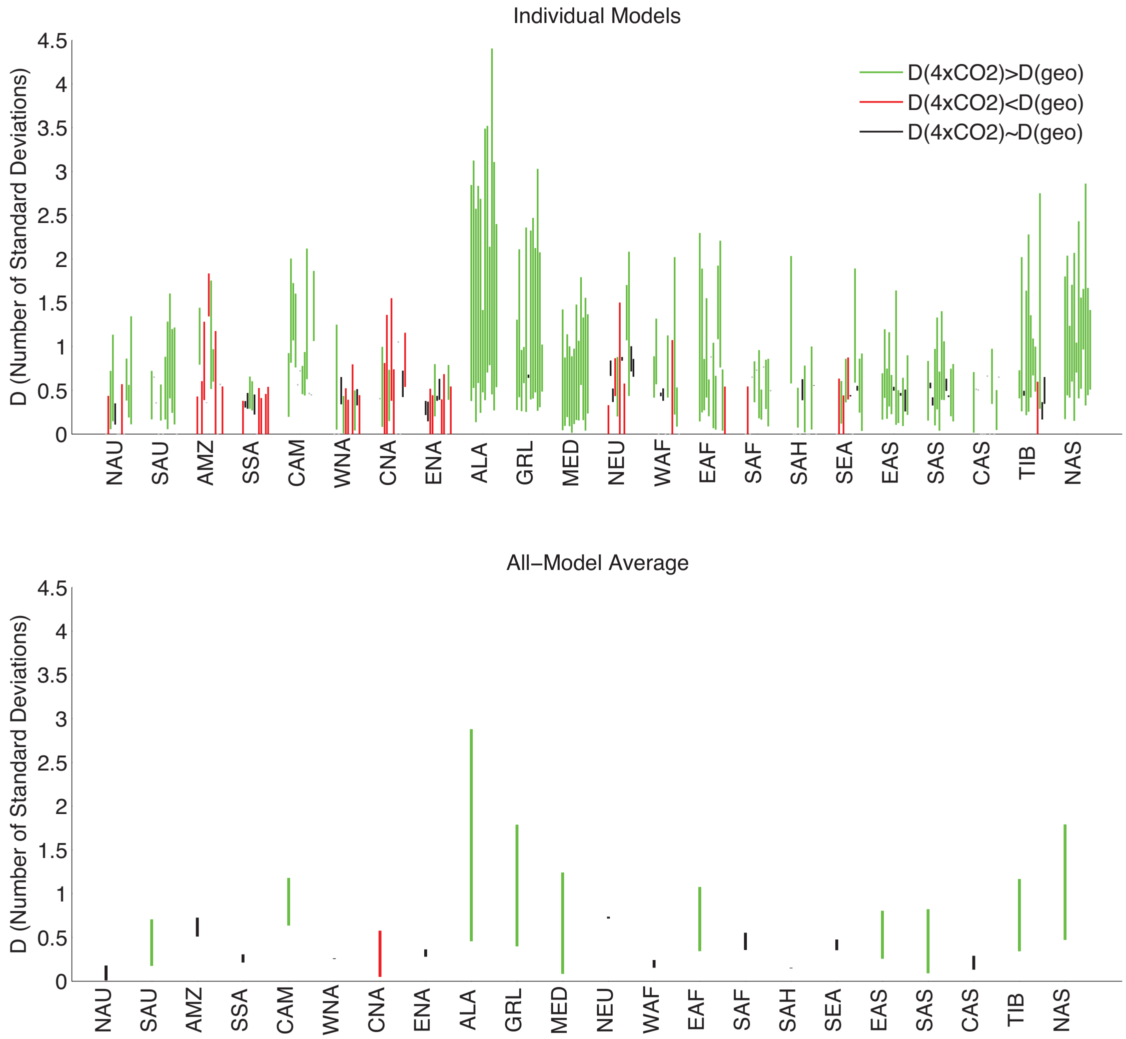

Figure 10: Changes in annual mean values of the climate change metric (D; Equation 3) for 100% of the weighting on precipitation ($w = 1$). Lines are drawn between the values of D for $g = 0$ (no geoengineering) and $g = 1$ (returning global mean temperature to the preindustrial value. In a given region (abscissa), green lines indicate individual model response (top panel) or all-model ensemble mean response (bottom panel) where D is greater for abrupt4xCO2 than for the reference level of solar reduction, red lines indicate where D is less for abrupt4xCO2 than for the reference level of solar reduction, and black lines indicate where the difference between $D_{\text{abrupt4xCO2}}$ and $D_{\text{reference}}$ is statistically insignificant (see Supplemental Section 1). Most of the regions show that geoengineering reduces precipitation D values from the D values for high CO_2. Analogous plots for 100% of the weighting on temperature are not shown, as all lines are green in all regions for all models.

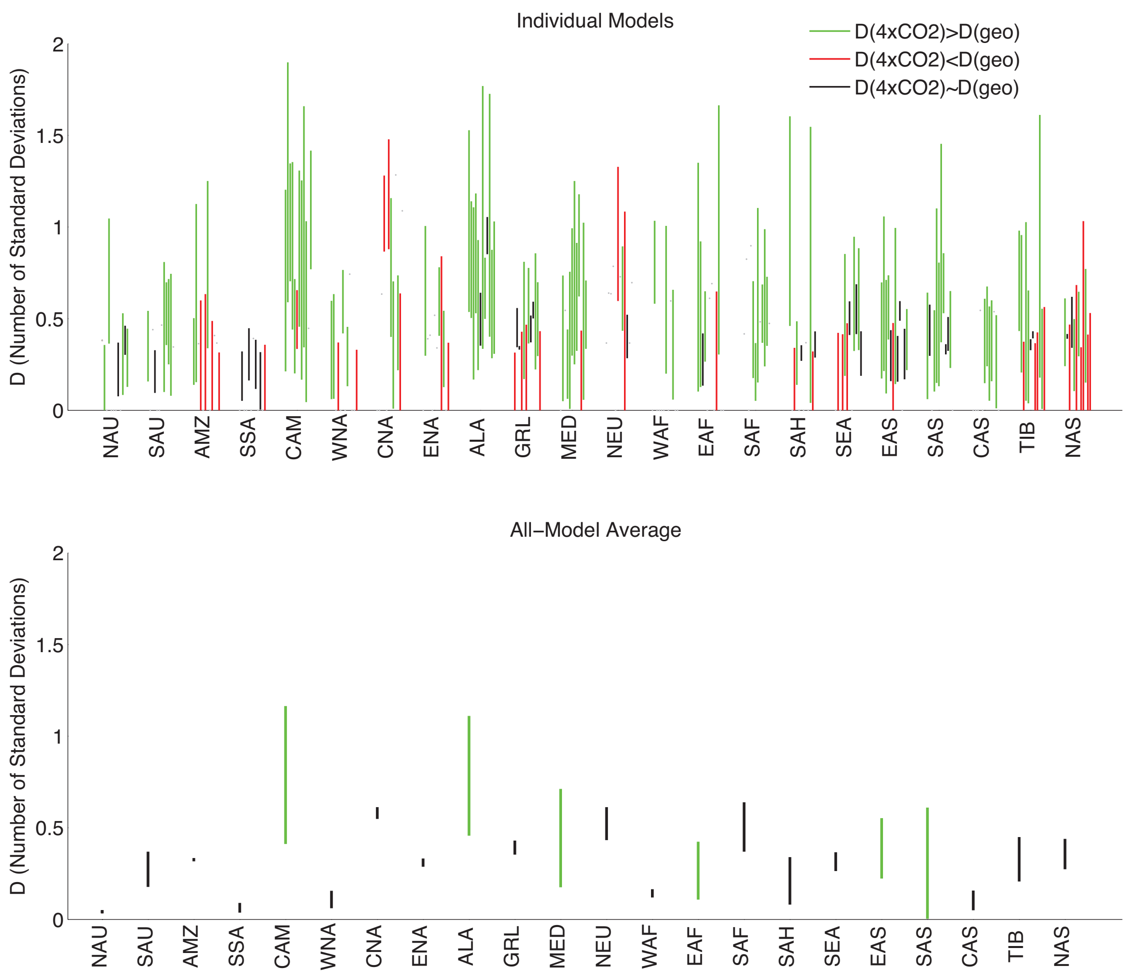

Figure 11: Same as Supplemental Figure 10, but for June-July-August averages. Most of the regions show that geoengineering reduces precipitation D values from the D values for high CO_2.

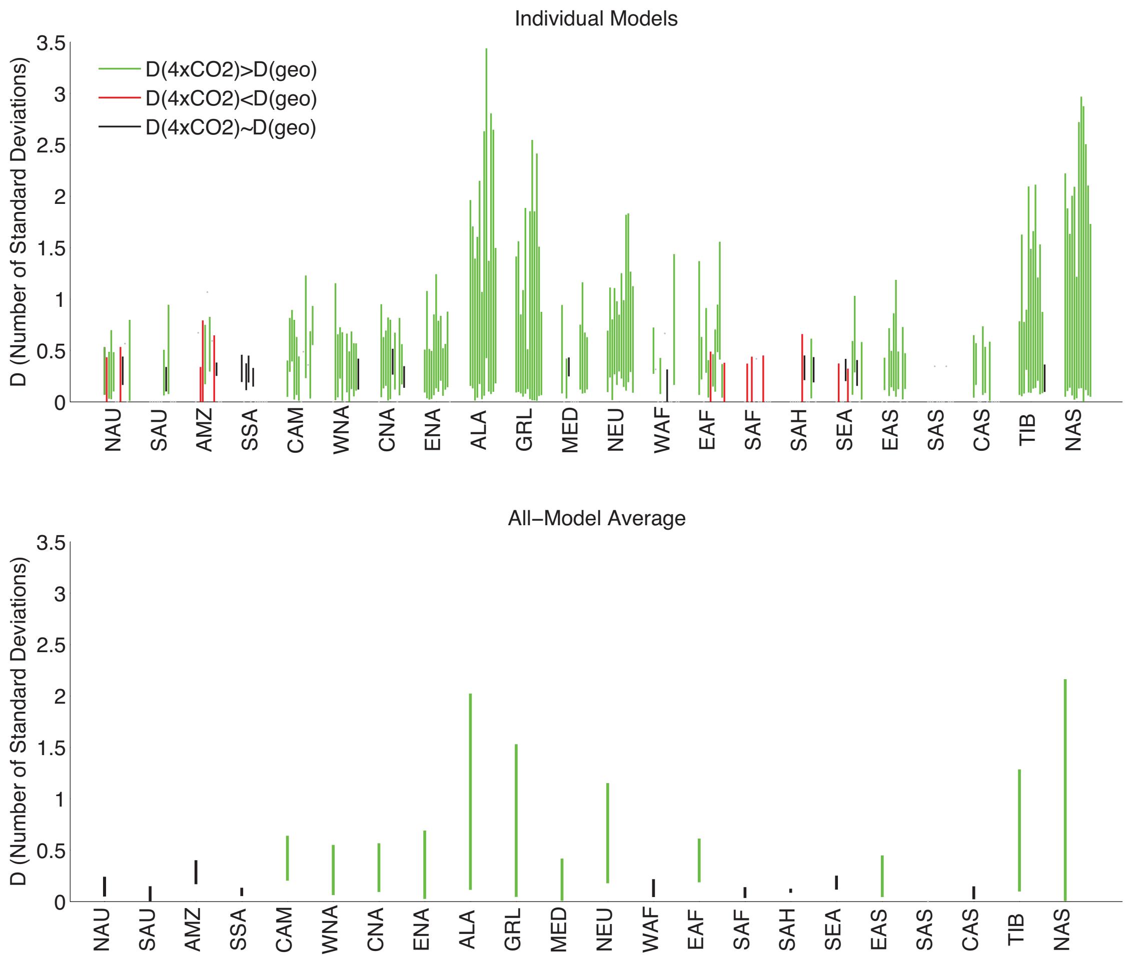

Figure 12: Same as Supplemental Figure 10, but for December-January-February averages. Most of the regions show that geoengineering reduces precipitation D values from the D values for high CO_2.

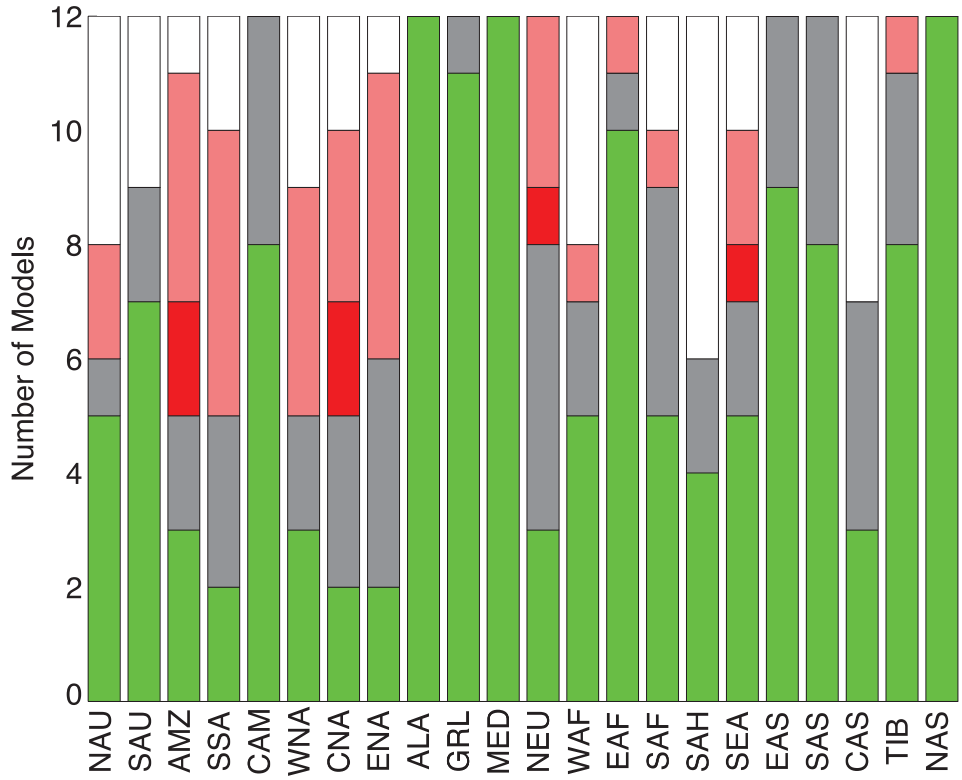

Figure 13: Bar chart characterizing annual mean values of D (Equation 3) for each region (abscissa). All values shown are for 100% of the weighting on precipitation ($w = 1$). Green indicates that $D(1;0) > D(1;1)$, or D for no geoengineering is greater than D for returning global mean temperature to the preindustrial value, i.e., geoengineering reduces D. Red indicates that $D(1;0) < D(1;1)$, i.e., geoengineering increases D. Grey indicates that the difference between $D(1;0)$ and $D(1;1)$ is statistically insignificant (see Supplemental Section 1), but $D(1;0)$ is statistically significant. Pale red indicates that $D(1;0)$ is not statistically significant, but $D(1;1)$ is statistically significant. White indicates that neither $g = 0$ nor $g = 1$ causes statistically significant changes in D. Analogous plots for 100% of the weighting on temperature are not shown, as all bars are green in all regions.

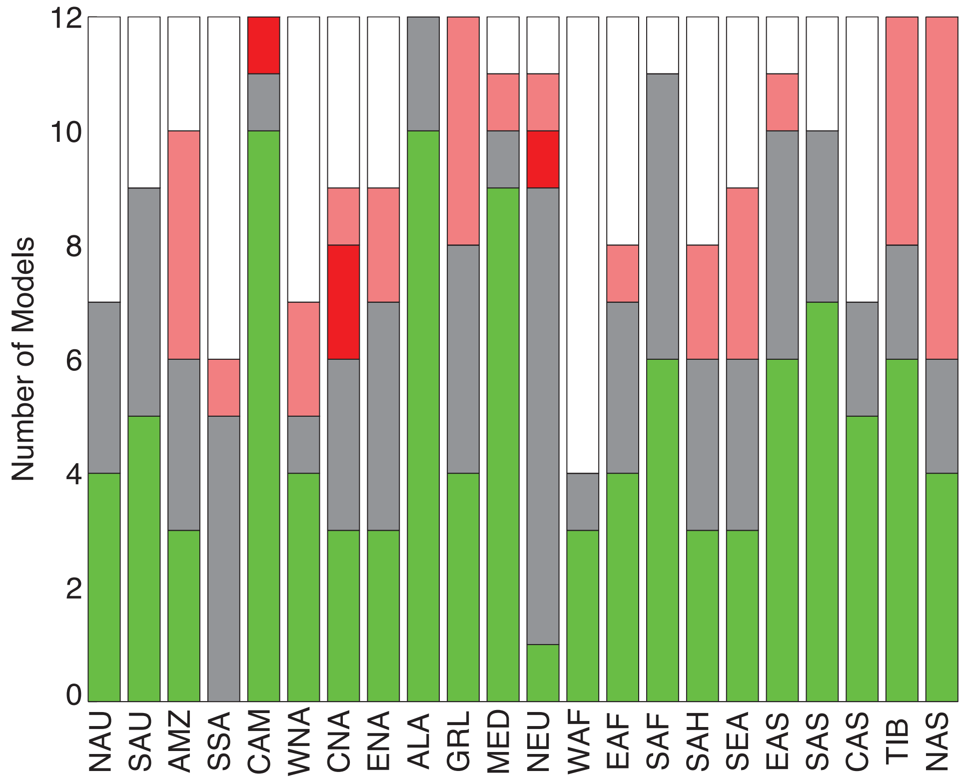

Figure 14: Same as Supplemental Figure 13, but for June-July-August averages.

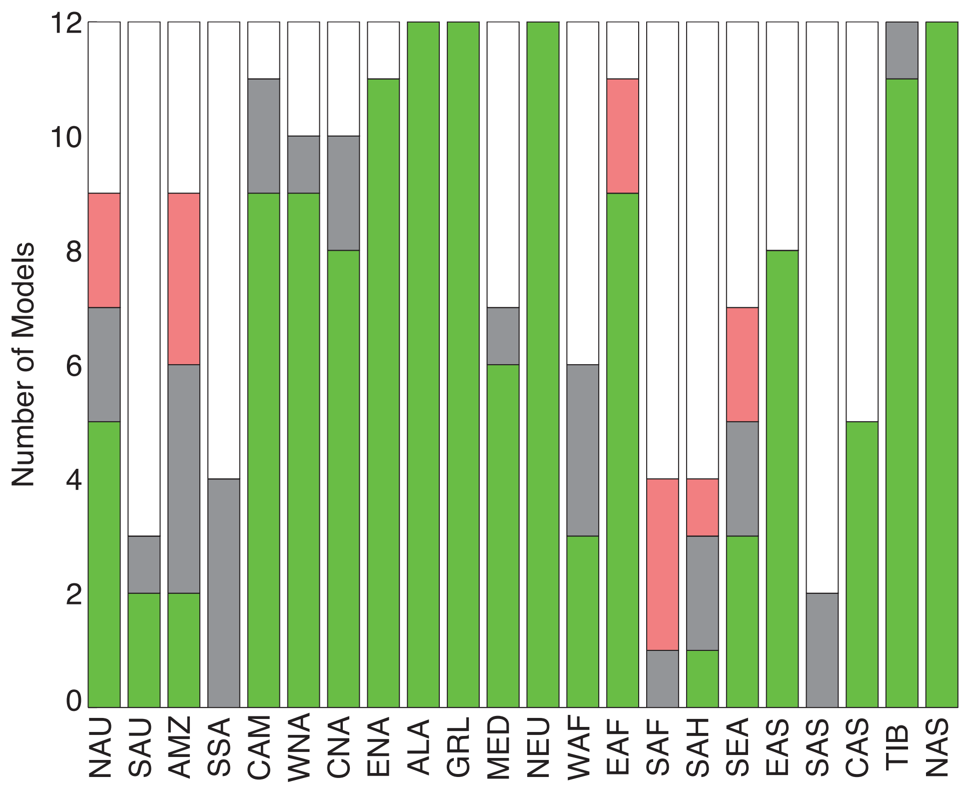

Figure 15: Same as Supplemental Figure 13, but for December-January-February averages.

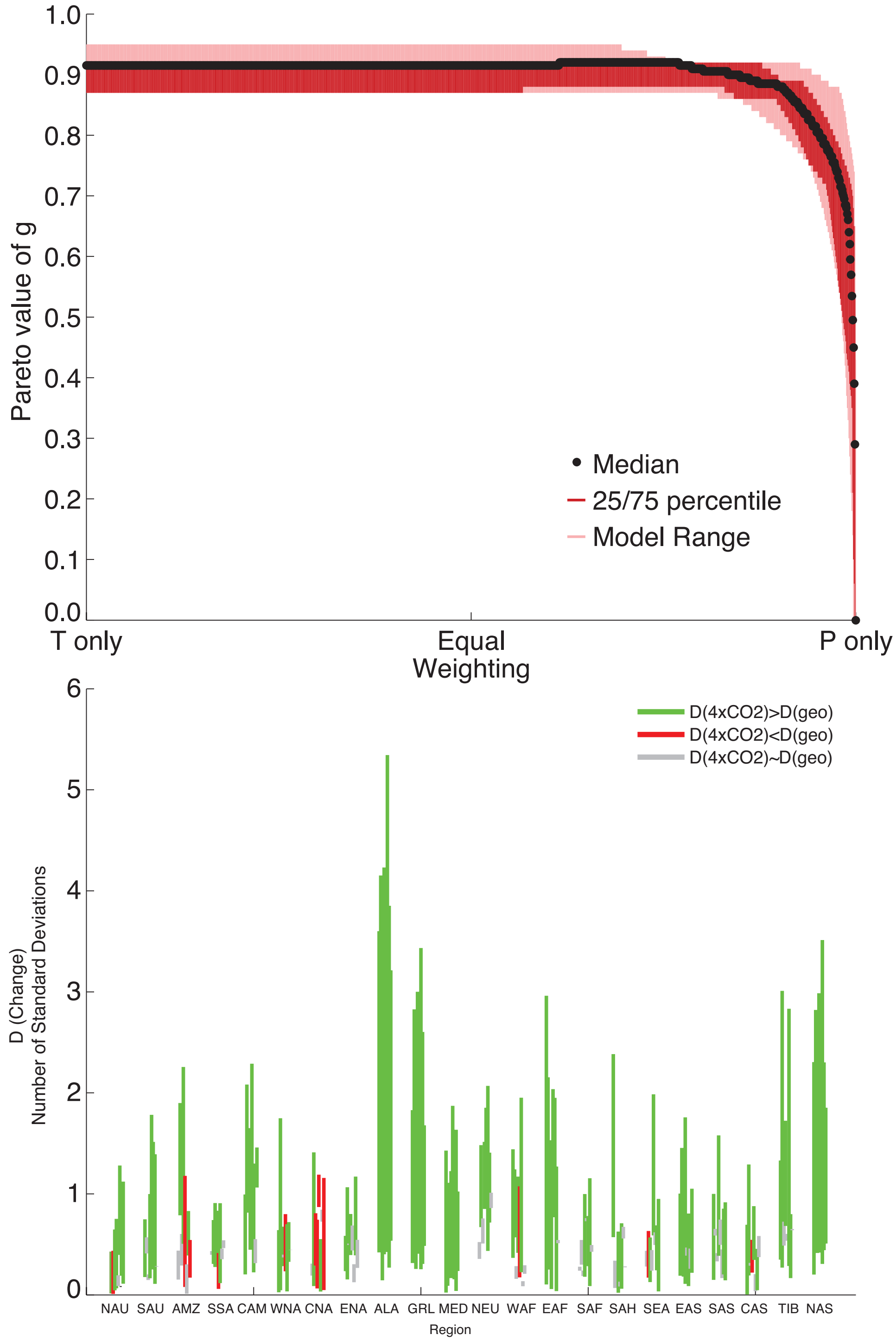

Figure 16: Top panel is same as Figure 3 in the main text, and bottom panel is same as the top panel of Supplemental Figure 10, where D values (Equation 3) for abrupt4xCO2 are calculated over an average of years 101-140 instead of years 11-50. See Supplemental Section 2 for motivation for this figure and further description. Essentially, averaging over a later period of abrupt4xCO2 does not change the results in this paper.